Comparing the Gauss-Seidel and Jacobi Relaxation Schemes in the Solution of the EHL Line Contact Problem Using a Multigrid solver

Janakiraman, Shravan; Klit, Peder

Publication date:
2014

Comparing the Gauss-Seidel and Jacobi Relaxation Schemes in the Solution of the EHL Line Contact Problem Using a Multigrid solver

S. Janakiraman[1]*, P. Klit[1]

[1]*Technical University of Denmark, Nils Koppels Alle, bld. 404, 2800 Kgs. Lyngby, Denmark.*

Abstract

The solution to the EHL line contact problem has been computed by building a multigrid solver. There are two types of relaxation schemes used in the solver, a Gauss -Seidel scheme and a combination of the Gauss-Seidel scheme and the Distributive Jacobi scheme. The differences in the convergence and residual norm values for each of the schemes is discussed.

Keywords: Multigrid, Jacobi, Gauss-Seidel.

*Corresponding author: Shravan Janakiraman (shja@mek.dtu.dk).

1. INTRODUCTION

Lubrecht[1] first solved the line and point contact EHL problem using a multigrid solution using a discretization based on the reduced pressure. Venner[2] then improved upon the solution to the EHL problem without using a reduced pressure approach. Venner also arrived at the solution using a combination of the Gauss-Seidel relaxation scheme and the distributive Jacobi relaxation scheme. Both Lubrecht and Venner used a fast multilevel, multi-integration method to calculate the nodal deformations described by Brandt and Lubrecht[3].Wang et al [4] developed a multigrid scheme without using the Full Approximation Scheme (FAS) right hand side value for the film thickness equation. This was made possible by assuming the film thickness to be dependent on the pressure and not treating it as an independent quantity. Wang used the deformation calculation scheme developed by Brandt and Lubrecht.

This paper studies the effects of using a mixed relaxation scheme (Gauss-Seidel and Jacobi) versus just a Gauss-Seidel scheme with small under-relaxation factors. The authors use a deformation calculation scheme developed by Houpert and Hamrock [5]. The FAS right hand side is not calculated as suggested by Wang [4].

2. THEORY

The basic equations necessary for solving Reynolds equation using the multigrid method are described [2].

$$L_i = \frac{1}{(\Delta X)^2}\left[\in_{\frac{i-1}{2}} P_{i-1} - \left(\in_{\frac{i-1}{2}} + \in_{\frac{i+1}{2}}\right) P_i + \in_{\frac{i+1}{2}} P_{i+1}\right] - \frac{1}{(\Delta X)}[H_i - H_{i-1}] = 0 \quad \text{(Eq 1)}$$

where $\in = \frac{H^3}{\mu\gamma}$, $\gamma = \frac{3\pi^2 U}{(4W^2)}$, i = (2….maxnode).

The dimensionless film thickness at a certain node is described by [5]

$$H_i = h_0 + \frac{X^2}{2} + \sum_{j=1}^{N} D_{i,j} P_j \quad \text{(Eq 2)}$$

The updated value of nodal pressure is given by

$$P_i^n = P_i^o + w_{gs}\delta_i \quad \text{(Eq 3)}$$

for the multigrid method solved purely by relaxing the equations at each level using a Gauss- Seidel scheme.

For the solver that uses a combination of the Gauss-Seidel scheme and the Distributive Jacobi scheme, the updated values of pressure are given by

$$P_i^n = P_i^o + w_{ja}(\delta_i - \delta_{i-1}) \quad \text{(Eq 4)}$$

in the Jacobi region and by (Eq 3) in the Gauss-Seidel region.

In the Gauss-Seidel region, δ_i is calculated as

$$\delta_i = \left(\frac{\partial L_i}{\partial P_i}\right)^{-1} r_i \quad \text{(Eq 5)}$$

In the Jacobi region of the mesh, δ_i is calculated as

$$\delta_i = \left(\frac{\partial L_i}{\partial P_i} - \frac{\partial L_i}{\partial P_{i-1}}\right)^{-1} r_i \quad \text{(Eq 6)}$$

$$\frac{\partial L_i}{\partial P_i} = -\frac{1}{(\Delta X)^2}\left[\left(\in_{\frac{i-1}{2}} + \in_{\frac{i+1}{2}}\right)\right] - \frac{1}{(\Delta X)}\left[D_{i,i} - D_{i-1,i}\right] \quad \text{(Eq 7)}$$

$$\frac{\partial L_i}{\partial P_i} - \frac{\partial L_i}{\partial P_{i-1}} = -\frac{1}{(\Delta X)^2}\left[\left(2 \in_{\frac{i-1}{2}} + \in_{\frac{i+1}{2}}\right)\right] - \frac{1}{(\Delta X)}\left[D_{i,i} - D_{i-1,i} - D_{i,i-1} + D_{i-1,i-1}\right] \quad \text{(Eq 8)}$$

The residual r_i is given by

$$r_i = F_i^k - \frac{1}{(\Delta X)^2}\left[\in_{\frac{i-1}{2}} P_{i-1}^n - \left(\in_{\frac{i-1}{2}} + \in_{\frac{i+1}{2}}\right) P_i^o + \in_{\frac{i+1}{2}} P_{i+1}^o\right] + \frac{1}{(\Delta X)}\left[H_i - H_{i-1}\right] \quad \text{(Eq 9)}$$

for the Gauss-Seidel region and

$$r_i = F_i^k - \frac{1}{(\Delta X)^2}\left[\in_{\frac{i-1}{2}} P_{i-1}^o - \left(\in_{\frac{i-1}{2}} + \in_{\frac{i+1}{2}}\right) P_i^o + \in_{\frac{i+1}{2}} P_{i+1}^o\right] + \frac{1}{(\Delta X)}\left[H_i - H_{i-1}\right] \quad \text{(Eq 10)}$$

for the Jacobi region.

A node is characterized as a node within the Gauss Seidel region if

$$\frac{\in_i}{(\Delta X)^2} > 1$$

and characterized as a Jacobi region node if it is not part of the Gauss Seidel region.

A Full Approximation Scheme (FAS) is used to solve the equations. W(1,2) cycles of different levels are run to achieve converged values of pressure and film thickness. The number of levels for which the W cycles are run are 4, 5 and 6. W(1,2) cycles are preferred to the usually used W(2,1) cycles because it was observed that the former method achieved faster convergence.

To transfer the pressure and FAS right hand side values from a fine mesh to a coarse mesh a full weighting restriction operator I_{k+1}^k is used

$$I_{k+1}^k = \frac{1}{4}[\,1\;2\;1] \quad \text{(Eq 11)}$$

Transferring the fine grid data

$$P^{o(k)} = I_{k+1}^k P^{n(k+1)} \quad \text{(Eq 12)}$$

$$F^k = L^k\left(I_{k+1}^k P^{n(k+1)}\right) + I_{k+1}^k\left(F^{k+1} - L^{k+1}P^{k+1}\right) \quad \text{(Eq 13)}$$

where $P^{o(k)}$ is the initial value of pressure on a grid at level k. $P^{n(k+1)}$ is the final value of pressure obtained at level k+1. F^k is the FAS RHS described by Venner [2] at level k. At the finest level (k = m), F^k is 0. k = 1 is the coarsest grid level.

To transfer the pressure values from a coarse mesh to a fine mesh a full weighting interpolation operator I_k^{k+1} is used

$$P^{o(k+1)} = P^{n(k+1)} + I_k^{k+1}\left(P^{n(k)} - I_{k+1}^k P^{n(k+1)}\right) \quad \text{(Eq 14)}$$

The value for h_0 is adjusted on the finest grid each W cycle. An under-relaxation factor of 0.001 is used for adjusting the value of h_0 .

On the finest level the force balance equation is

$$\frac{1}{2}\Delta X^m \sum_{j=1}^{maxnode}\left(P_j^m + P_{j+1}^m\right) = \frac{\pi}{2} \quad \text{(Eq 15)}$$

where m refers to the finest grid level.

The following pressure convergence criterion is used

$$error_p = \left(\frac{\sum_{j=1}^{maxnode} |P_i^n - P_i^o|}{\sum_{j=1}^{maxnode} P_i^o}\right) < 0.001 \quad \text{(Eq 16)}$$

W(1,2) cycles are run for a 4 level system with the number of nodes at the finest level being 241 and the coarsest level 31. 3 relaxations are applied on the mesh at the coarsest level. Convergence is studied when using just the Gauss-Seidel scheme and a combination of both the Gauss-Seidel and the Jacobi relaxation schemes.

The algorithm describing the number of relaxations involved at each level is described by Wang[4].

3. RESULTS & DISCUSSION

W(1,2) cycles are run for a combination of the Gauss-Seidel and the Jacobi relaxation schemes. The Gauss-Seidel scheme is used mainly in the inlet where the value of the viscosity is not relatively high. The Jacobi scheme is used in the Hertzian contact width where the pressure values are large enough to cause a large viscosity gradient.

(**Fig. 1**) shows the convergence of the multigrid method for varying values of the Jacobi under-relaxation factors.

The number of W(1,2) cycles required for convergence in increasing order of the under-relaxation values shown in the graph are 356, 313, 289, 292 and 292 cycles respectively. The Jacobi under-relaxation factor 0.4 converges the fastet. w_{ja} values of 0.5 and 0.6 converge marginally slower than than a value of $w_{ja} = 0.4$ (**Fig. 5**). Convergence is not obtained for w_{ja} values greater than 0.6.

W(1,2) cycles are also run for a relaxation scheme using just the Gauss-Seidel method. These cycles were run on the same 4 grid levels as earlier, with the number of nodes on the finest grid being 241. The results are shown in (**Fig. 3**), and (**Fig. 4**).

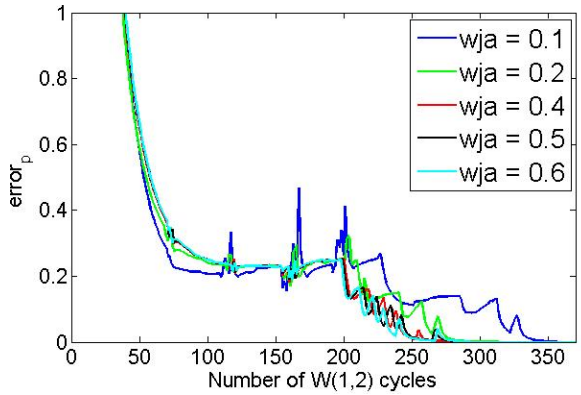

Figure 1 : *Convergence of the Reynolds equation for varying values of* w_{ja}.

(**Fig. 2**) shows the residual norm of of the finest level at the end of each W cycle. The residual norm (rn) is defined as

$$rn = \frac{1}{maxnode-1}\sum_{i=1}^{maxnode-1}|r_i| \qquad \text{(Eq 19)}$$

where $|r_i|$ is the absolute value of the residual at node i.

The rn values drop rapidly for about the first 100 W cycles and then stagnate or slightly increase before dropping off again. The flattening of each rn curve occurs around the same W cycle region as the flattened convergence curves in (**Fig. 1**). This seems to suggest that the stagnation of the residual norm values plays a role in the stagnation of the convergence curves.

(**Fig. 3**) shows the number of W cycles required for convergence as the Gauss-Seidel under-relaxation factors w_{gs} are increased. The number of cycles required at w_{gs} values of 0.1, 0.2 and 0.3 are 1276, 716 and 514 respectively. This is expected as a smaller under-relaxation factor updates the solution relatively slowly as compared to the higher under-relaxation factors. Convergence is not obtained for w_{gs} values of 0.4 and above.

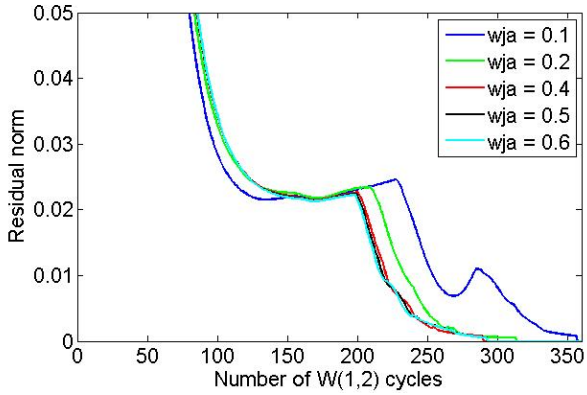

Figure 2 : *Residual norm for varying values of wja using a mixed relaxation scheme*

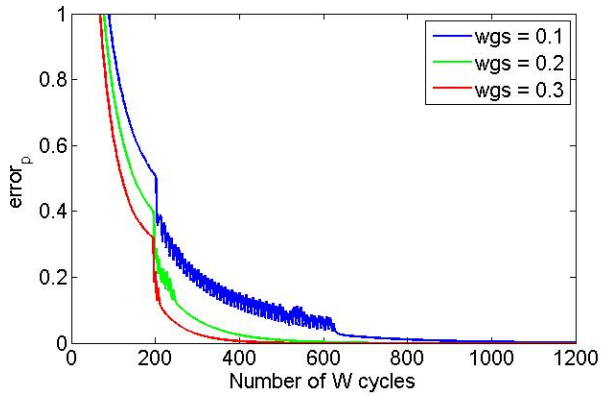

Figure 3 : *Convergence of Reynolds equation for varying values of wgs using only a Gauss Seidel relaxation scheme*

Wang[4] had stated that using just a Gauss-Seidel relaxation scheme leads to faster convergence than using a mixed relaxation scheme because the Jacobi relaxation slows down convergence. However these results show that using optimum Gauss-Seidel and Jacobi relaxation values leads to a faster convergence than the fastest converging Gauss-Seidel solution.

(**Fig. 4**) shows the rn curves for a 4 level W(1,2) cycle using only a Gauss-Seidel relaxation scheme. These curves are much more conventional in that the residual norm decreases faster as the under-relaxation factor is increased. This is also reflected in the convergence curves in (**Fig. 3**)

The fastest converging curves for each relaxation scheme are plotted in (**Fig. 6**). The mixed relaxation scheme converges much faster for about the first 75 cycles before flattening out until about the 200th W cycle. Both the curves once again increase their convergence rate after about 200 W cycles. These

curves show that the Gauss-Seidel scheme converges slower than the mixed relaxation scheme.

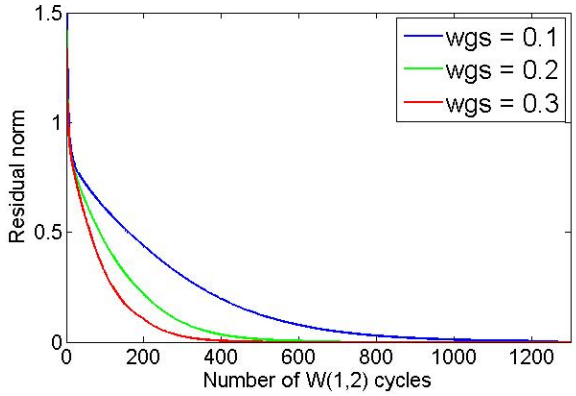

***Figure 4** : Residual norm for varying values of wgs using a Gauss-Seidel relaxation scheme*

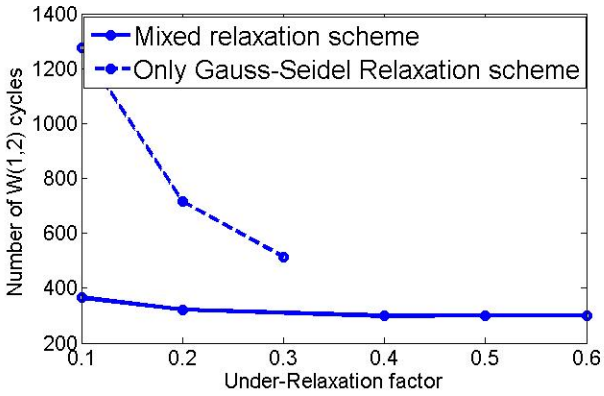

***Figure 5** : Comparison of the number of W(1,2) cycles to convergence for the 2 relaxation schemes*

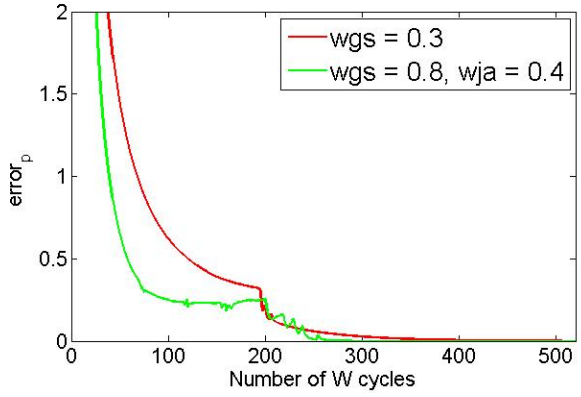

***Figure 6** : Comparison of the convergence of the two relaxation schemes*

W(1,2) cycles are also run for 3 separate maximum levels for the multigrid. The levels are 4, 5 and 6. The minimum number of nodes at each level is 31. The maximum number of nodes at each level is 241, 481 and 961 respectively.

(**Fig. 7**) shows the convergence patterns of the 3 different levels of multigrid solutions using a mixed relaxation scheme. As the mesh becomes finer, the accuracy of the solution increases. However lower frequency components of the error are introduced, thus increasing convergence time. (**Fig. 7**) also shows that there is no fixed w_{ja} value at which the fastest convergence can be reached. There seems to be an optimum value of w_{ja} and w_{gs} at which fastest convergence can be achieved .

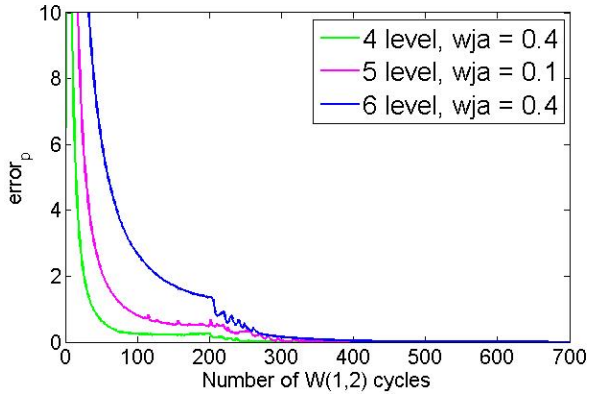

***Figure 7 :** Comparison of the convergence of varying multigrid levels incorporated in a W(1,2) cycle for a mixed relaxation scheme with w_{gs} = 0.8 .*

(**Fig. 8**) compares the residual norm of the mixed relaxation scheme for each of the 4 level, 5 level and 6 level multigrid. The 4 level solution converges after 289 W cycles, the 5 level solution at 418 cyles and the 6 level solution at 670 cycles.

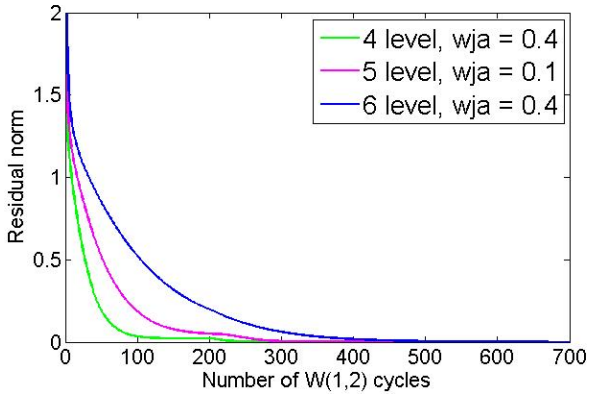

***Figure 8:** Residual norm for the 3 levels of multigrid solutions using a mixed relaxation scheme with w_{gs} = 0.8.*

5 level and 6 level multigrid solutions are also plotted using just a Gauss-Seidel relaxation scheme. Given that it is easier to predict the Gauss-Seidel under-

relaxation value at which the solution converges the fastest, a value of 0.3 was chosen.

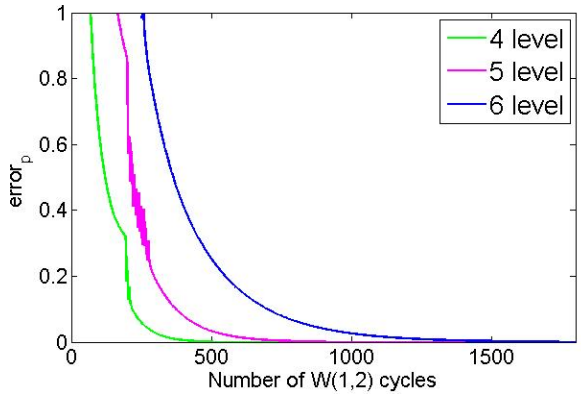

Figure 9: *Convergence curves for the 3 levels of multigrid solutions using a Gauss-Seidel relaxation scheme with w_{gs} = 0.3*

The multigrid solution with the finest scheme produces the slowest converging solution as expected (**Fig. 9**). The 4 level solution converges after 506 W cycles, the 5 level after 911 cycles and the 6 level solution after 1743 cycles.

The rn curves for the Gauss-Seidel solution for the 3 levels of solution is shown in (**Fig. 10**).

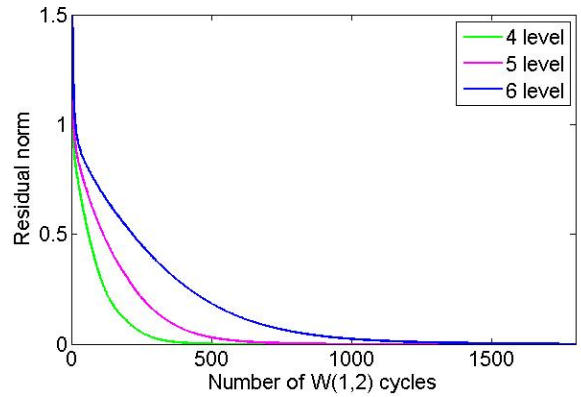

Figure 10: *Residual norm for the 3 levels of multigrid solutions using a mixed relaxation scheme with w_{gs} = 0.3.*

A 4 level multigrid solution is also run with the number of nodes on the finest level being 81 and the coarsest level being 11. The fastest converging solution was obtained for w_{ja} = 0.5 and w_{gs} = 0.1 . The solution converged after 371 W(1,2) cycles. Converging solutions were not obtained at w_{ja} values less than 0.5. This fastest converging solution (green curve) is plotted against the fastest converging 4 level solution, having 241 nodes as it's finest grid (pink curve) (**Fig. 11**).

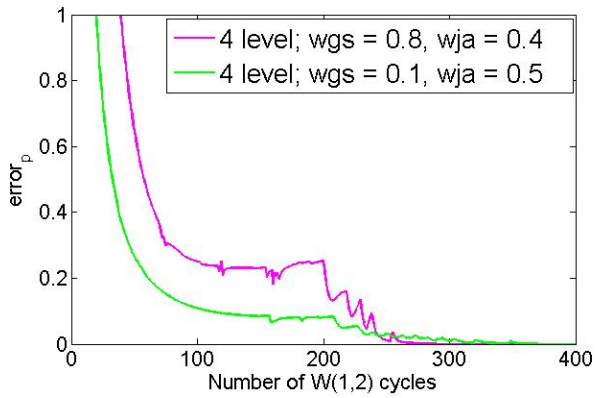

Figure 11: *Convergence curves for the two different 4 level solutions.*

The pink curve in (**Fig. 11**) refers to the 4 level solution with the coarsest grid having 31 nodes and the finest grid having 241 nodes. The green curve refers to the solution having 11 nodes at the coarsest level and 81 nodes at the finest level. The rn curves for the same solution is plotted in (**Fig. 12**). The curves are interesting because the green curve initially converges faster than the pink curve, but then flattens out and reaches convergence slower than the pink curve.

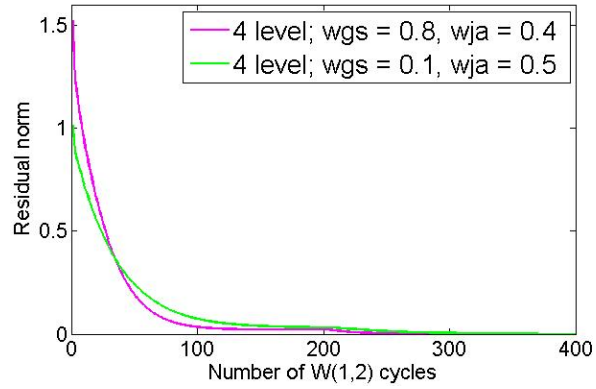

Figure 12: *Residual norm for the two different 4 level solutions.*

Thus the pink curve reaches convergence requiring a lower number of W cycles (289) as compared to the green curve (371). But given that each W cycle on the green curve requires a far computation than the pink curve, it takes far lesser time to achieve convergence on the system with the finest frid being 81 nodes and the coarsest grid being 11 nodes.

However as we approach a grid system where the finest level consists of a relatively small number of nodes, there is a loss in accuracy at the finest level.
The converged pressure spike values for the grid system having 81 nodes on the finest level and 241 nodes at the finest level are compared to the theoretical

pressure spike values predicted by Hamrock and Pan [6] in (**Fig. 13**) .

The theoretical value of the pressure spike for W' = 1.42e-4, U = 8.16e-12, G = 5007 is P_s = 0.659.

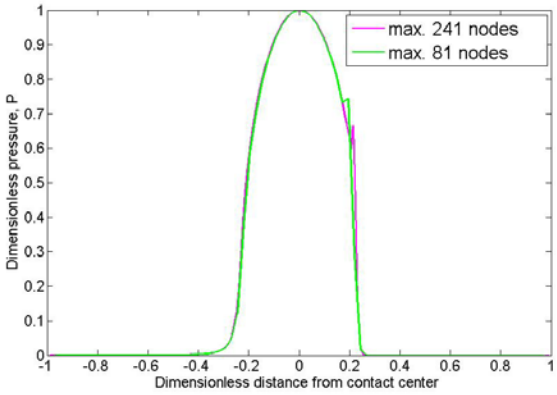

Figure 13: *Converged pressure curves for the two different 4 level solutions.*

The error in the pressure spike value for the system having 81 nodes on the finest level is 11.31% . The error for the system with 241 nodes on its finest level is 0.75% .

4. CONCLUSIONS

W(1,2) cycles are run to provide a multigrid solution to the EHL line contact problem.

- A relaxation scheme using a combination of the Gauss-Seidel scheme for the inlet region and the Jacobi scheme for the Hertzian region converges faster than a relaxation scheme using just the Gauss-Seidel method.
- A 4 level multigrid solution converges faster than a 6 level multigrid solution. This is because the larger number of nodes in the finest level of the 6 level solution introduce low frequency errors that decrease the convergence rate.
- For a multigrid solution using a mixed relaxation scheme, it is not straightforward to predict the combination of under-relaxation factors that lead to the fastest converging solution.
- For a multigrid solution using just the Gauss-Seidel relaxation scheme, the convergence rate increases with an increasing under-relaxation factor.
- For two 4 level multigrid solutions, the solution having a larger number of nodes on the finest level is more accurate than the solution having smaller number of nodes on the finest level.

5. NOMENCLATURE

b	Hertzian half contact width
E	equivalent Young's Modulus, Pa
G	Material Constant
H	dimensionless film thickness
P	dimensionless pressure, p/p_h
P_i^n	Newest value of dimensionless pressure
P_i^o	dimensionless pressure at previous step
p_h	Maximum Hertzian pressure, Pa
R	equivalent radius, m
U	dimensionless velocity parameter, $u\mu_0/ER$
u	lubricant inlet velocity, m/s
W'	dimensionless load
μ_0	ambient viscosity of lubricant, Pas
μ	dimensionless viscosity
w_{ja}	Jacobi under-relaxation factor
w_{gs}	Gauss-Seidel under-relaxation factor

6. REFERENCE

1. A.A. Lubrecht, W.E. Ten Napel, R. Bosma, Multigrid an alternative method for calculating film thickness and pressure profiles in elastohydrodynamically lubricated line contacts. ASME J Tribol 1986;108
2. C.H.Venner, Multilevel solution of the EHL line and point contact problems. Enschede: PhD thesis, university of Twente, Netherlands 1991..
3. A. Brandt, A.A.Lubrecht, Multilevel matrix multiplication and fast solution of integral equations. J Comput Phys 1990;90.
4. J. Wang, S. Qu, P. Yang, Simplified multigrid technique for the numerical solution to the steady-state and transient EHL line contacts and the arbitrary entrainment EHL point contacts. Tribology international 34 (2001), 191-202.
5. L.G. Houpert and B.J. Hamrock, Fast approach for calculating film thicknesses and pressures in elastohydrodynamically lubricated contacts at high loads. J. Tribol., vol. 108, 110.
6. B.J. Hamrock, P. Pan, R.T. Lee, Pressure spikes in elastohdrodynamically lubricated conjunctions. J. Tribol., vol. 110, no. 2, pp 279-284